APPROXIMATE BAYESIAN INFERENCE WITH STEIN FUNCTIONAL VARIATIONAL GRADIENT DESCENT

Anonymous authors
Paper under double-blind review

ABSTRACT

We propose a general-purpose variational algorithm that forms a natural analogue of Stein variational gradient descent (SVGD) in function space. While SVGD successively updates a set of particles to match a target density, the method introduced here of Stein functional variational gradient descent (SFVGD) updates a set of particle functions to match a target stochastic process (SP). The update step is found by minimizing the functional derivative of the Kullback-Leibler divergence between SPs. SFVGD can either be used to train Bayesian neural networks (BNNs) or for ensemble gradient boosting. We show the efficacy of training BNNs with SFVGD on various real-world datasets.

1 INTRODUCTION

Bayesian inference can be treated as a powerful framework for data modeling and reasoning under uncertainty. However, this assumes that we can encode our prior knowledge in a meaningful manner. Typically, this is done by specifying the prior distribution of the model parameters. However, in machine learning (ML), models potentially consist of millions of parameters with potentially highly complex interactions (e.g., very large neural networks (NNs)). Furthermore, the parameter structure of the models itself is allowed to change during training, e.g., the number of parameter grows when using gradient boosting (GB). This makes defining meaningful prior assumptions for parameter spaces difficult or nearly (practically) infeasible. As we usually do not care about single parameters but the complete resulting function, it seems intuitive to directly express our prior knowledge in hypothesis function space by, e.g., specifying the characteristic length scale, periodicity, or smoothness in general. Fortunately, Bayesian inference can also be formulated in function space. In this case, the prior and posterior distributions are stochastic processes (SPs). The most prominent representative is the Gaussian process (GP), for which the posterior GP can be analytically computed. However, training GPs scale cubically in the number of observations, and the implicit Gaussian likelihood assumption is often violated in reality.

In this paper, we introduce Stein functional variational gradient descent (SFVGD). This method provides a general gradient descent method in function space that enables practitioners to train ML models to approximate the posterior SP, assuming certain regularity conditions of the prior SP and the likelihood function hold.

1.1 RELATED WORK

Kernelized Stein Methods These methods combine Stein's identity with a reproducing kernel Hilbert space (RKHS) assumption. Based on a finite particle set, they can either be used to find the optimal transport direction to match a target density or to estimate the score gradient of the empirical distribution of the particles. The former is called Stein variational gradient descent (SVGD) Liu & Wang (2016), and approaches of the latter category are called (non-parametric) score estimators (Zhou et al., 2020). Our method internally uses SVGD and forms a natural analogue in function space. Several extensions to SVGD exist, e.g., approaches incorporating second-order information such as Leviyev et al. (2022) and the more general matrix-kernel valued approach by Wang et al. (2019a). While these extensions usually outperform SVGD, their computational costs are also higher.

Bayesian Neural Networks (BNNs) Typically, BNNs are NNs with weight priors that are trained via variational inference. The prominent representatives are BNNs using *Bayes by Backprop* (Blundell

et al., 2015) and scalable probabilistic backpropagation (Hernandez-Lobato & Adams, 2015). Recently, Immer et al. (2020) proposed transforming BNNs into generalized linear models with inference based on a Gaussian process equivalent to the model. While Markov Chain Monte Carlo (MCMC) methods often are prohibitively expensive to be used for BNNs, some variants, e.g., Chen et al. (2014) account for noisy gradient evaluations and can be used in this setting. However, MCMC-based methods are still usually employed for relatively low-dimensional problems.

Functional BNNs (FBNNs) Sun et al. (2019) proposed to use functional priors to train BNNs. Training BNNs with our descent is closely related to their method, but while they use a score-based approach for the estimation of the derivative of the Kullback-Leibler divergence D_{KL} between the prior SP and the variational SP, we estimate this derivative directly via SVGD. Wang et al. (2019b) also use SVGD for FBNNs but apply SVGD directly to the D_{KL} between the posterior SP and the variational SP. Furthermore, their work does not show that this in fact maximizes a lower bound for the log marginal likelihood. Recently, Ma & Hernández-Lobato (2021) and Rudner et al. (2021) proposed different FBNN approaches that also build upon the results of Sun et al. (2019), but while their methods are specific to training NN function generators, our method can be used to update a set of particle functions in general.

Repulsive Deep Ensembles Repulsive Deep Ensembles are deep ensembles that incorporate repulsive terms in their gradient update, forcing their members' weights apart. A variety of repulsive terms are presented in (D'Angelo & Fortuin, 2021) and (D'Angelo et al., 2021), outperforming the approach by Wang et al. (2019b). However, these approaches mainly focus on weight priors, and empirical findings also only relate to the weight space. In contrast to our work, functional priors can only be applied if a posterior SP with analytical marginal density exists.

GB with Uncertainty The closest neighbor of our approach applied to GB is the ensemble GB scheme proposed by Malinin et al. (2021), which is based on Bayesian ensembles. Hence, in contrast to our functional approach, their method is based on approximating the posterior of the model parameters.

1.2 Our contribution

We propose a novel natural extension of SVGD in function space (Section 3), which enables the practitioner to match a target SP. This approach can be implemented in a BNN or as a GB routine, as derived in Section 3.3. Using real-world data benchmarks, we show that the resulting generator training algorithm is competitive while having less computational costs than the approach of Sun et al. (2019). In contrast to other existing uncertainty-aware GB algorithms, a GB ensemble, when trained via SFVGD, can naturally incorporate prior functional information. These versatile applications of our framework are made possible by providing a unifying view of NNs and GB from a functional analysis perspective.

2 Background

2.1 Supervised ML from a functional analysis perspective

Given a labeled dataset $\mathcal{D} \in (\mathcal{X} \times \mathcal{Y})^n \sim \mathbb{P}^n_{\mathbf{x}y}$ of $n \in \mathbb{N}$ independent and identically distributed (i.i.d.) observations from an unknown data generating process $\mathbb{P}_{\mathbf{x}y}$, a supervised ML algorithm tries to construct a risk optimal model f under a pre-specified loss L. In this case, the function f defines a mapping from the feature space $\mathcal{X}$ to the target space $\mathcal{Y}$. The learning algorithm $\mathcal{I}$ to construct f is a function mapping from the set of all datasets $\bigcup_{n\in\mathbb{N}}(\mathcal{X} \times \mathcal{Y})^n$ to a hypothesis space $\mathcal{H}$, which is a subset of the set of all functions mapping from $\mathcal{X}$ to the model output space[1] $\widetilde{\mathcal{Y}} \subset \mathbb{R}^g$ with $g \in \mathbb{N}$. In order to specify the goodness-of-fit of a function f, one can define a loss function $L : \mathcal{Y} \times \widetilde{\mathcal{Y}} \to \mathbb{R}, (y, f(\mathbf{x})) \mapsto L(y, f(\mathbf{x}))$, which measures how well the output of a fixed model $f \in \mathcal{H}$ fits an observation $(\mathbf{x}, y) \sim \mathbb{P}_{\mathbf{x}y}$. In the following, we present supervised ML from a functional analysis perspective. Here, we fix the observation and associate the loss L with the loss functional$L_{(\mathbf{x},y)}[f] : \mathcal{H} \to \mathbb{R}, f \mapsto L(y, f(\mathbf{x}))$. Based on this loss functional, we can define the risk functional of a model f,

$$\mathcal{R}[f] = \mathbb{E}_{(\mathbf{x},y)\sim\mathbb{P}_{\mathbf{x}y}} L_{(\mathbf{x},y)}[f], \tag{1}$$

[1] If $\mathcal{Y}$ is numeric, $\widetilde{\mathcal{Y}} = \mathcal{Y}$. Otherwise, $\widetilde{\mathcal{Y}}$ is a numerical encoding of $\mathcal{Y}$.

which measures the expected loss of f, and is used to theoretically identify optimal models. In the following, we will assume that the expectation in Eq. (1) exists and is finite. If we knew the usually unknown data generating process and hence the risk functional, we could update any model $f \in \mathcal{H}$ in the direction of the steepest descent in $\mathcal{H}$ w.r.t. $\mathcal{R}$ by following the negative functional gradient of $\mathcal{R}$. The negative functional gradient of $\mathcal{R}$, $-\nabla_f \mathcal{R}[f]$, is itself a mapping from $\mathcal{X}$ to $\widetilde{\mathcal{Y}}$. For every input location $\mathbf{x}$, this gradient returns the direction in model output space $\widetilde{\mathcal{Y}}$, which points to the locally steepest descent w.r.t. $\mathcal{R}$. In the following, unless otherwise stated, the functional derivative is taken in the L^2 space.

Proposition 2.1 *Assuming sufficient regularity and that $L(y, f(\mathbf{x}))$ is partially continuously differentiable w.r.t. $f(\mathbf{x})$, we observe for numeric inputs and model output that*

$$-\nabla_f \mathcal{R}[f](\mathbf{x}) = -p_{\mathbf{x}}(\mathbf{x}) \cdot \mathbb{E}_{y \sim \mathbb{P}_{y|\mathbf{x}}} \frac{\partial L(y, f(\mathbf{x}))}{\partial f(\mathbf{x})}, \tag{2}$$

where $p_{\mathbf{x}}$ is the marginal density of $\mathbf{x}$.

The proof is given in A.1.1. In practice, we usually do not know $p_{\mathbf{x}}$, and since our dataset $\mathcal{D}$ is finite, we only have access to n realizations of $\frac{\partial L(y, f(\mathbf{x}))}{\partial f(\mathbf{x})}$. If the feature space is at least partially continuous, its size $|\mathcal{X}| = \infty$, and we thus cannot estimate $-\nabla_f \mathcal{R}[f](\mathbf{x})$ without additional assumptions. However, we have access to the functional empirical risk $\mathcal{R}_{\text{emp},\mathcal{D}}[f] := \sum_{(\mathbf{x}_i, y_i) \in \mathcal{D}} L_{(\mathbf{x}_i, y_i)}[f]$, for which we assume that it converges in mean to $\mathcal{R}$ as $n \to \infty$. Its negative functional gradient can be expressed via the chain rule such that

$$-\nabla_f \mathcal{R}_{\text{emp},\mathcal{D}}[f](\mathbf{x}) = -\sum_{(\mathbf{x}_i, y_i) \in \mathcal{D}} \frac{\partial L(y_i, f(\mathbf{x}_i))}{\partial f(\mathbf{x}_i)} \cdot \nabla_f \left[f(\mathbf{x}_i)\right](\mathbf{x}), \tag{3}$$

where $\nabla_f \left[f(\mathbf{x}_i)\right]$ is the functional gradient of the evaluation functional of f at $\mathbf{x}_i$, which evaluates to the Dirac delta function $\delta_{\mathbf{x}_i}$. However, since we take the functional gradient in $\mathcal{H}$, $\nabla_f \left[f(\mathbf{x}_i)\right]$ becomes the projection of $\delta_{\mathbf{x}_i}$ into $\mathcal{H}$. For example, if $\mathcal{H}$ is an RKHS with associated kernel k, then $\nabla_f \left[f(\mathbf{x}_i)\right](\mathbf{x}) = k(\mathbf{x}_i, \mathbf{x})$, i.e., our choice of $\mathcal{H}$ directly influences the "bumpiness" of $\nabla_f \mathcal{R}_{\text{emp},\mathcal{D}}[f]$. Furthermore, we can interpret $\nabla_f \mathcal{R}_{\text{emp},\mathcal{D}}[f]$ as a (jump-)continuous functional representation of the dataset $\partial \mathcal{D}_{L,f} := \{(\mathbf{x}_i, -\frac{\partial L(y_i, f(\mathbf{x}_i))}{\partial f(\mathbf{x}_i)}) \big| \, (\mathbf{x}_i, y_i) \in \mathcal{D}\} \subset (\mathcal{X} \times \widetilde{\mathcal{Y}})^n$, which also implicitly defines a learner. In the following, we show how two of the core supervised ML algorithms – namely, gradient boosting and neural networks – naturally incorporate this functional gradient while training.

Gradient Boosting (GB) For GB, the situation is usually reversed, and we choose a (base) learner $\mathcal{I}_b$ that implicitly defines $\mathcal{H}$ and with which we fit a model to the data set $\partial \mathcal{D}_{L,f}$. GB uses these approximations of the negative functional gradient of the empirical risk to successively update a model $f^{[0]}$ such that

$$f^{[t+1]} = f^{[t]} + \eta^{[t]} b^{[t]} \text{ with } b^{[t]} = \mathcal{I}_b(\partial \mathcal{D}_{L,f^{[t]}}), \tag{4}$$

where $\eta^{[t]} \in \mathbb{R}_{>0}$ is the learning rate and possibly depends on the iteration $t \in \mathbb{N}$.

Neural Networks (NNs) If f is an NN with parameters $\boldsymbol{\phi}$, then the parameter gradients w.r.t. the empirical risk functional needed for backpropagation can be obtained via the chain rule such that

$$\begin{aligned} \nabla_{\boldsymbol{\phi}} \mathcal{R}_{\text{emp},\mathcal{D}}[f] &= \int_{\mathcal{X}} \nabla_f \mathcal{R}_{\text{emp},\mathcal{D}}[f](\mathbf{x}) \cdot \nabla_{\boldsymbol{\phi}} f(\mathbf{x}) \mathrm{d}\mathbf{x} \\ &= \sum_{(\mathbf{x}_i, y_i) \in \mathcal{D}} \frac{\partial L(y_i, f(\mathbf{x}_i))}{\partial f(\mathbf{x}_i)} \cdot \nabla_{\boldsymbol{\phi}} f(\mathbf{x}_i), \end{aligned} \tag{5}$$

where the second equality holds, since here we do not restrict $\mathcal{H}$, i.e., $\nabla_f \left[f(\mathbf{x}_i)\right] = \delta_{\mathbf{x}_i}$.

However, these procedures only assure that we can find an optimal model $f \in \mathcal{H}$ w.r.t. $\mathcal{R}_{\text{emp}}$, which does not imply that f is optimal w.r.t. $\mathcal{R}$. In practice, we tune the hyperparameters of the algorithms – i.e., use data withheld from learning for subsequent model selection – and apply early stopping to find a model f approximately optimal w.r.t. $\mathcal{R}$.

2.2 STOCHASTIC PROCESSES

In this section, we will shortly introduce stochastic processes (SPs) that can be used to represent distributions over functions and thereby allow us to express the uncertainty of models independent of their specific parameter structure. We will regard $\mathcal{X}$ as an index set and let $(\mathcal{Y}, \mathcal{G})$ be a measurable space with σ-algebra $\mathcal{G}$ on the state space $\mathcal{Y}$. For $\mathbf{x} \in \mathcal{X}$ and a given probability space $(\Omega, \mathcal{F}, \mathbb{P})$ based on the sample space Ω, $\mathcal{F}$ is a σ-algebra on Ω and probability measure $\mathbb{P}$. Let $Q(\mathbf{x})$ be a random variable projecting from Ω to $\mathcal{Y}$. An SP Q is the family $\{Q(\mathbf{x});\ \mathbf{x} \in \mathcal{X}\}$ of all random variables $Q(\mathbf{x})$ (Lamperti, 1977). With this, we can define a sample function $f_\omega : \mathcal{X} \to \mathcal{Y}, \mathbf{x} \mapsto Q(\mathbf{x})(\omega)$ for a fixed $\omega \in \Omega$. Often, it is easier to look at SPs from this sample function view: For every $A \in \mathcal{F}$, a set of functions $\{f_\omega;\ \omega \in A\}$ with an associated measure $\mathbb{P}(A)$ can be identified – i.e., SPs define a distribution over functions projecting from $\mathcal{X}$ to $\mathcal{Y}$. For a finite index set $\mathbf{X} := \mathbf{x}_{1:m} \in \mathcal{X}^m$, we denote the finite-dimensional marginal joint distribution over function values $\{Q(\mathbf{x}_1), \dots, Q(\mathbf{x}_m)\}$ as $Q_\mathbf{X}$. In the following, we assume that for every $Q_\mathbf{X}$ exists a corresponding density function $p_{Q_\mathbf{X}} : \mathcal{Y}^m \to \mathbb{R}_{\geq 0}, \mathbf{f}^\mathbf{X} \mapsto p_{Q_\mathbf{X}}(\mathbf{f}^\mathbf{X})$, where $\mathbf{f}^\mathbf{X} := (f(\mathbf{x}_1), \dots, f(\mathbf{x}_m))$ are the function values at $\mathbf{x}_{1:m}$ based on a sample function f where we suppressed the ω to ease the following notation. We will denote the associated functional to this density function with $p_{Q_\mathbf{X}}[f]$.

The D_{KL} is a measure of distance between two distributions over the same probability space. Since SPs are distributions over functions, the D_{KL} can also be used for distances between two SPs. Unfortunately, computing this quantity is non-trivial (Matthews et al., 2015). However, for two consistent and ergodic SPs Q and P, i.e., Q and P can be characterized by marginals over all finite index sets (e.g., GPs), Sun et al. (2019) showed that the D_{KL} between these SPs can be solely expressed in terms of their marginals, i.e.,

$$D_{\mathrm{KL}}(Q||P) = \sup_{m \in \mathbb{N}, \mathbf{X} \in \mathcal{X}^m} D_{\mathrm{KL}}(Q_\mathbf{X} \| P_\mathbf{X}). \tag{6}$$

This expression enables us to find a differentiable distance measure between two stochastic processes.

2.3 STEIN VARIATIONAL GRADIENT DESCENT

SVGD (Liu & Wang, 2016) is a variational Bayesian method. Variational methods can be used to approximate the generally intractable posterior density of a continuous random variable $\boldsymbol{\theta}$

$$p_{\theta|\mathcal{D}}(\boldsymbol{\theta}) = \frac{p_{\mathcal{D}|\boldsymbol{\theta}}(\mathcal{D}|\boldsymbol{\theta}) p_{\boldsymbol{\theta}}(\boldsymbol{\theta})}{\int p_{\mathcal{D}|\boldsymbol{\theta}}(\mathcal{D}|\boldsymbol{\theta}) p_{\boldsymbol{\theta}}(\boldsymbol{\theta}) \mathrm{d}\boldsymbol{\theta}}, \tag{7}$$

where $p_{\mathcal{D}|\boldsymbol{\theta}}$ and $p_{\boldsymbol{\theta}}$ are the likelihood and the prior density function, respectively. SVGD tries to match the posterior $p_{\boldsymbol{\theta}|\mathcal{D}}$ with a density q represented via a fixed number $r \in \mathbb{N}$ of pseudo-samples – so-called particles – and iteratively updates them by minimizing $D_{\mathrm{KL}}(q \| p_{\boldsymbol{\theta}|\mathcal{D}}) = \int q(\boldsymbol{\theta}) \frac{\log(q(\boldsymbol{\theta}))}{p_{\boldsymbol{\theta}|\mathcal{D}}(\boldsymbol{\theta})} d\boldsymbol{\theta}$. In an RKHS with associated kernel k, the optimal update direction is found by considering the negative functional derivative

$$-\nabla_f D_{\mathrm{KL}}(q_{[T]} \| p_{\boldsymbol{\theta}|\mathcal{D}})\big|_{f=0} = \mathbb{E}_{\boldsymbol{\theta} \sim q}\left[\nabla_{\boldsymbol{\theta}} \log p_{\boldsymbol{\theta}|\mathcal{D}}(\boldsymbol{\theta}) k(\boldsymbol{\theta}, \cdot) + \nabla_{\boldsymbol{\theta}} k(\boldsymbol{\theta}, \cdot)\right], \tag{8}$$

where $T(\boldsymbol{\theta}) = \boldsymbol{\theta} + f(\boldsymbol{\theta})$, and $q_{[T]}$ is the density of $\boldsymbol{\theta}' = T(\boldsymbol{\theta})$ when $\boldsymbol{\theta} \sim q$. We can estimate this functional gradient based on the particles in an unbiased manner, as we are able to evaluate the score function of $p_{\boldsymbol{\theta}|\mathcal{D}}$ (i.e., $\nabla_{\boldsymbol{\theta}} \log p_{\boldsymbol{\theta}|\mathcal{D}}$), although $\log p_{\boldsymbol{\theta}|\mathcal{D}}$ might be intractable.

3 STEIN FUNCTIONAL VARIATIONAL GRADIENT DESCENT

In this section, we develop a functional version of SVGD which we will call *Stein functional variational gradient descent* (SFVGD). While SVGD can be used to approximate the posterior distribution of a continuous random variable, SFVGD can be applied when we are interested in the posterior SP $P_{f|\mathcal{D}}$ defined by its Radon-Nikodym derivative (Schervish, 1995) w.r.t. the prior SP P_f,

$$\frac{dP_{f|\mathcal{D}}}{dP_f}[f] = \frac{p_{\mathcal{D}|f}[\mathcal{D}|f]}{\int p_{\mathcal{D}|f}[\mathcal{D}|f] dP_f[f]}, \tag{9}$$

where $p_{\mathcal{D}|f}$ is the likelihood functional, which measures how likely it is to observe $\mathcal{D}$, given a sample function f. In the following, we assume that the posterior $P_{f|\mathcal{D}}$ exists and also that it is an ergodic and consistent SP. Analogously to SVGD, we try to approximate $P_{f|\mathcal{D}}$ with a distribution Q represented by pseudo-samples. However, for SFVGD, these particles are now functions.

3.1 OBJECTIVE FUNCTION

Since analytical solutions for the differential Eq. (9) only exist in special cases (e.g., if the prior P_f is a GP and the likelihood is also Gaussian), we use the D_{KL} between two SPs to formulate an optimization objective. More specifically, the goal of our framework is to construct an approximating measure Q^* for which it holds that

$$Q^* \in \operatorname*{arg\,min}_{Q \in \mathcal{Q}} D_{\mathrm{KL}}(Q \| P_{f|\mathcal{D}}), \tag{10}$$

where $\mathcal{Q}$ is the set of representable variational posterior processes. Here, we represent Q via $r \in \mathbb{N}$ sample functions $f_1, \ldots, f_r$ from Q, which act as pseudo-samples and which we also call particle functions. It can be shown (Matthews et al., 2015) that minimizing Eq. (10) is equivalent to maximizing the functional evidence lower bound (ELBO) $\mathcal{L}_{\mathcal{D}}$, i.e.,

$$Q^* \in \operatorname*{arg\,max}_{Q \in \mathcal{Q}} \underbrace{\mathbb{E}_{f \sim Q}\left[\ell[\mathcal{D}|f]\right] - D_{\mathrm{KL}}(Q \| P_f)}_{=:\mathcal{L}_{\mathcal{D}}(Q)}, \tag{11}$$

where $\ell[\mathcal{D}|f] := \log p_{\mathcal{D}|f}[\mathcal{D}|f]$. The advantage of formulation (11) over (10) is that Eq. (11) only depends on known quantities. In the following, we apply Eq. 6, i.e., the results of Sun et al. (2019) regarding the D_{KL} of ergodic and consistent SPs, yielding

$$Q^* \in \operatorname*{arg\,max}_{Q \in \mathcal{Q}} \inf_{m \in \mathbb{N}, \mathbf{X} \in \mathcal{X}^m} \underbrace{\mathbb{E}_{f \sim Q}[\ell[\mathcal{D}|f]] - D_{\mathrm{KL}}(Q_{\mathbf{X}} \| P_{f_{\mathbf{X}}})}_{=:\mathcal{L}_{\mathcal{D},\mathbf{X}}(Q)}. \tag{12}$$

In contrast to Sun et al. (2019), however, we do not unfold the D_{KL} term, since we are able to directly take its functional gradient via SVGD. The resulting maximin game formulation of Eq. (12) proves to be challenging to solve, especially since we need to minimize over discrete sets $\mathbf{X}$ and the infimum also does not ensure a finite m. Hence, we follow Sun et al. (2019) by replacing the inner minimization with a sampling-based approach, i.e.,

$$Q^* \in \operatorname*{arg\,max}_{Q \in \mathcal{Q}} \mathbb{E}_{\mathcal{D}_s} \mathbb{E}_{\mathbf{X}_M \sim C_{\mathcal{X}}} \left[\mathcal{L}_{\mathcal{D}_s, [\mathbf{X}_{\mathcal{D}_s}, \mathbf{X}_M]}(Q)\right], \tag{13}$$

where $\mathcal{D}_s$ is a random subsample of size $|\mathcal{D}_s| = s$ drawn from $\mathcal{D}$. $\mathbf{X}_{\mathcal{D}_s}$ are the associated feature vectors of $\mathcal{D}_s$, and $\mathbf{X}_M = [\mathbf{x}_1, \ldots, \mathbf{x}_M]^\top \in \mathcal{X}^M$ are M stacked random feature vectors drawn from a sampling distribution $C_{\mathcal{X}}$ with support $\mathcal{X}$. If $\mathcal{X}$ is bounded, Sun et al. (2019) proposes a uniform distribution for $C_{\mathcal{X}}$. It has been shown in Sun et al. (2019) for $\mathcal{D}_s = \mathcal{D}$ and $M > 1$ that $\mathcal{L}_{\mathcal{D}, [\mathbf{X}_{\mathcal{D}}, \mathbf{X}_M]}$ is a lower bound for the log marginal likelihood $\log p(\mathcal{D})$, i.e., the maximization in Eq. 13 implies the minimization in Eq. 10. Although, as noted by Burt et al. (2020), if $\mathcal{Q}$ is a parametric family, the objective is ill-defined, we did not encounter problems in practice. Also, we could straightforwardly use the grid functional D_{KL} proposed by Ma & Hernández-Lobato (2021), which fixes some of these theoretical shortcomings. However, also note that SFVGD itself does not assume $\mathcal{Q}$ to be parametric.

3.2 FUNCTIONAL DERIVATIVE OF THE OBJECTIVE

When using conventional gradient descent methods, we want to apply a map to update the parameters of our model such that our loss is reduced. In SFVGD, we proceed in a similar manner but update functions towards a loss-minimizing direction. A map that takes a function as an argument and returns another function is called an operator. Hence, we want to express how our objective value Eq. 13 changes when an operator $F : \mathcal{H} \to \mathcal{H}, f \mapsto f_F$ is applied to every $f \sim Q$. This means that the objective value changes with F such that

$$\mathcal{L}_{\mathcal{D}_s, \mathbf{X}}(Q_{[T]}) = \mathbb{E}_{\widetilde{f} \sim Q_{[T]}} \ell[\mathcal{D}_s|f] - D_{\mathrm{KL}}(Q_{[T]\mathbf{X}} \| P_{f_{\mathbf{X}}}), \tag{14}$$

where $T(f) = f + F(f)$ and $Q_{[T]}$ is the distribution of $\widetilde{f} = T(f)$ when $f \sim Q$. Naturally, we are interested in the functional derivative of Eq. 14 w.r.t. to F, since this gives us the direction of the steepest ascent in operator space regarding the functional ELBO. However, in order to make our computations tractable, we must limit the space of feasible operators:

Definition 3.1 *Let $F : \mathcal{H} \to \mathcal{H}, f \mapsto f_F$ be a continuous operator with the property that for all $m \in \mathbb{N}$ and each $\mathbf{X} \in \mathcal{X}^m$ exists a function $F_{\mathbf{X}} : \mathcal{Y}^m \to \mathcal{Y}^m$ such that $\mathbf{f}_F^{\mathbf{X}} = F_{\mathbf{X}}(\mathbf{f}^{\mathbf{X}})$ for any $f \in \mathcal{H}$.We call such an operator "evaluation-only dependent".*

Thus, F does not depend on derivatives of f (which is not a restriction, since we only assumed f to be continuous); we can also treat F as a construction rule of $F_{\mathbf{X}}$ for arbitrary m and $\mathbf{X}$. Now, we can state the functional gradient of the objective functional w.r.t. an evaluation-only dependent operator F, for $\mathbf{X} = [\mathbf{X}_{\mathcal{D}_s}, \mathbf{X}_M]$ and $\widetilde{\mathbf{X}} = \mathbf{X}_{\mathcal{D}_s}$

$$\begin{aligned}\nabla_F \mathcal{L}_{\mathcal{D}_s,\mathbf{X}}(Q_{[T]}) &= \nabla_F \mathbb{E}_{\widetilde{f}\sim Q_{[T]}} \ell[\mathcal{D}_s|\widetilde{f}] - \nabla_F D_{\mathrm{KL}}(Q_{[T]_{\mathbf{X}}} \| P_{f_{\mathbf{X}}}) \\ &= \nabla_F \mathbb{E}_{\widetilde{\mathbf{y}}\sim Q_{[T]_{\widetilde{\mathbf{X}}}}} \ell(\mathcal{D}_s, \widetilde{\mathbf{y}}) - \nabla_F D_{\mathrm{KL}}(Q_{[T]_{\mathbf{X}}} \| P_{f_{\mathbf{X}}}),\end{aligned} \tag{15}$$

where we assumed that there exists a log-likelihood function $\ell : \bigcup_{s\in\mathbb{N}} (\mathcal{X}\times\mathcal{Y})^s \times \mathcal{Y}^s \to \mathbb{R}$ such that $\ell[\mathcal{D}_s|f] = \ell(\mathcal{D}_s, \mathbf{f}^{\widetilde{\mathbf{X}}})$ for every $\mathcal{D}_s$. If we set $F = 0$, then T becomes the identity operator, i.e. $Q_{[T]} = Q$. Since we want to iteratively update our particle functions, we must only consider small perturbations around $F = 0$.

Proposition 3.1 *For an evaluation-only dependent operator F, the functional derivative of the functional ELBO at $F = 0$ evaluated for a function f*

$$\begin{aligned}\nabla_F \mathcal{L}_{\mathcal{D}_s,\mathbf{X}}(Q_{[T]})\big|_{F=0}(f) = &\ \mathbb{E}_{\widetilde{\mathbf{y}}\sim Q_{\widetilde{\mathbf{X}}}} \left[\nabla_{\widetilde{\mathbf{y}}} \ell(\mathcal{D}_s, \widetilde{\mathbf{y}}) \cdot \delta_{\widetilde{\mathbf{y}}}(\mathbf{f}^{\widetilde{\mathbf{X}}})\right] \cdot \left[\delta_{\widetilde{\mathbf{X}}_1}(\cdot), \ldots, \delta_{\widetilde{\mathbf{X}}_s}(\cdot)\right]^\top \\ &+ \ \mathbb{E}_{\mathbf{y}\sim Q_{\mathbf{X}}} \left[\nabla_{\mathbf{y}} \log p_{P_{f_{\mathbf{X}}}}(\mathbf{y}) k_{\mathbf{Y}}(\mathbf{y}, \mathbf{f}^{\mathbf{X}}) + \nabla_{\mathbf{y}} k_{\mathbf{Y}}(\mathbf{y}, \mathbf{f}^{\mathbf{X}})\right] \\ &\cdot \left[\delta_{\mathbf{X}_1}(\cdot), \ldots, \delta_{\mathbf{X}_{s+M}}(\cdot)\right]^\top,\end{aligned} \tag{16}$$

where we assume that $\mathcal{H}_{\mathbf{Y}} \subset \{f : \mathcal{Y}^{s+M} \to \mathcal{Y}^{s+M}\}$ is an RKHS with associated kernels $k_{\mathbf{Y}}$.

The proof is given in A.1.2, where we also show the following corollary.

Corollary 3.1.1 *For an evaluation-only dependent operator F, the functional derivative of the functional ELBO at $F = 0$ evaluated for a function f*

$$\begin{aligned}\nabla_F \mathcal{L}_{\mathcal{D}_s,\mathbf{X}}(Q_{[T]})\big|_{F=0}(f) = &\ \mathbb{E}_{\widetilde{\mathbf{y}}\sim Q_{\widetilde{\mathbf{X}}}} \left[\nabla_{\widetilde{\mathbf{y}}} \ell(\mathcal{D}_s, \widetilde{\mathbf{y}}) \cdot k_{\widetilde{\mathbf{Y}}}(\widetilde{\mathbf{y}}, \mathbf{f}^{\widetilde{\mathbf{X}}})\right] \cdot \left[\delta_{\widetilde{\mathbf{X}}_1}(\cdot), \ldots, \delta_{\widetilde{\mathbf{X}}_s}(\cdot)\right]^\top \\ &+ \ \mathbb{E}_{\mathbf{y}\sim Q_{\mathbf{X}}} \left[\nabla_{\mathbf{y}} \log p_{P_{f_{\mathbf{X}}}}(\mathbf{y}) k_{\mathbf{Y}}(\mathbf{y}, \mathbf{f}^{\mathbf{X}}) + \nabla_{\mathbf{y}} k_{\mathbf{Y}}(\mathbf{y}, \mathbf{f}^{\mathbf{X}})\right] \\ &\cdot \left[\delta_{\mathbf{X}_1}(\cdot), \ldots, \delta_{\mathbf{X}_{s+M}}(\cdot)\right]^\top,\end{aligned} \tag{17}$$

where we assume that $\mathcal{H}_{\mathbf{Y}} \subset \{f : \mathcal{Y}^{s+M} \to \mathcal{Y}^{s+M}\}, \mathcal{H}_{\widetilde{\mathbf{Y}}} \subset \{f : \mathcal{Y}^s \to \mathcal{Y}^s\}$ are RKHSs with associated kernels $k_{\mathbf{Y}}, k_{\widetilde{\mathbf{Y}}}$, respectively.

We call $\nabla_F \mathcal{L}_{\mathcal{D}_s,\mathbf{X}}(Q_{[T]})\big|_{F=0}$ the Stein functional variational gradient operator. It inherits its name from SVGD, which internally is used to find the functional derivative of the D_{KL} term. The key idea of SFVGD is that by updating every particle function $f \sim Q$ via functional gradient descent in the direction of $\nabla_F \mathcal{L}_{\mathcal{D}_s,\mathbf{X}}(Q_{[T]})\big|_{F=0}(f)$, we carry out a gradient step in the distribution space. This increases the current overall functional ELBO value we want to maximize by pulling Q closer to Q^* and consequently also closer to the true posterior stochastic process $P_{f|\mathcal{D}}$.

3.3 Algorithms

Based on the particle functions $f_1, \ldots, f_r$, we can find an estimator of Eq. 16

$$\begin{aligned}\widetilde{\nabla}_F \mathcal{L}_{\mathcal{D}_s,\mathbf{X}}(Q_{[T]})\big|_{F=0}(f) = &\ \frac{1}{r}\sum_{i=1}^{r} \left[\nabla_{\mathbf{f_i}^{\widetilde{\mathbf{X}}}} \ell(\mathcal{D}_s, \mathbf{f_i}^{\widetilde{\mathbf{X}}}) \delta_{\mathbf{f_i}^{\widetilde{\mathbf{X}}}}(\mathbf{f}^{\widetilde{\mathbf{X}}})\right] \cdot \left[\delta_{\widetilde{\mathbf{X}}_1}(\cdot), \ldots, \delta_{\widetilde{\mathbf{X}}_s}(\cdot)\right]^\top \\ &+ \ \frac{\lambda}{r}\sum_{i=1}^{r} \left[\nabla_{\mathbf{f_i}^{\mathbf{X}}} \log p_{P_{f_{\mathbf{X}}}}(\mathbf{f_i}^{\mathbf{X}}) k_{\mathbf{Y}}(\mathbf{f_i}^{\mathbf{X}}, \mathbf{f}^{\mathbf{X}}) + \nabla_{\mathbf{f_i}^{\mathbf{X}}} k_{\mathbf{Y}}(\mathbf{f_i}^{\mathbf{X}}, \mathbf{f}^{\mathbf{X}})\right] \\ &\cdot \left[\delta_{\mathbf{X}_1}(\cdot), \ldots, \delta_{\mathbf{X}_{s+M}}(\cdot)\right]^\top,\end{aligned} \tag{18}$$

where we introduce a regularization parameter $\lambda \in \mathbb{R}_{\geq 0}$. Furthermore, if we set $\lambda = 1$, the estimator becomes an unbiased estimator of Eq. (16). Since $\mathcal{L}_{\mathcal{D},\mathbf{X}}$ is a lower bound of the log marginal likelihood $\log p(\mathcal{D})$, it would be preferable to update the particle functions via $\widetilde{\nabla}_F \mathcal{L}_{\mathcal{D},\mathbf{X}}(Q_{[T]})\big|_{F=0}$.

However, the major computation bottleneck in Eq. 18 is the calculation of the score gradient $\nabla_{\mathbf{f_i}\mathbf{x}} \log p_{P_{f_\mathbf{X}}}(\mathbf{f_i}^\mathbf{X})$ for all particle functions $f_i,\ i = 1, \dots, r$ evaluated at $\mathbf{X}$. For example, if P_f is a GP, then the costs of computing $\nabla_{\mathbf{f_i}\mathbf{x}} \log p_{P_{f_\mathbf{X}}}(\mathbf{f_i}^\mathbf{X})$ are $\mathcal{O}((s+M)^3 r)$. In addition, the computation of all kernel values $k_\mathbf{Y}(\mathbf{f_i}^\mathbf{X}, \mathbf{f_j}^\mathbf{X}),\ i = 1, \dots, r,\ j = 1, \dots, r$ required in Eq. 18 costs $\mathcal{O}(r^2)$. However, this is usually small compared to the cost of computing the score gradient for the functional prior. We choose for M a small constant number, since $\mathcal{L}_{\mathcal{D},[\mathbf{X}_\mathcal{D},\mathbf{X}_M]}$ is a lower bound for the log marginal likelihood $\log p(\mathcal{D})$ for $M > 1$, and we set r to a number of particle functions that can represent the posterior SP reasonably well. Thus, we are interested in estimating $\widetilde{\nabla}_F \mathcal{L}_{\mathcal{D},\mathbf{X}}(Q_{[T]})\big|_{F=0}$ with mini-batches. In principle, an unbiased estimate of $\ell(\mathcal{D}, \mathbf{f_i}^{\mathbf{X}_\mathcal{D}})$ is $n/s \cdot \ell(\mathcal{D}_s, \mathbf{f_i}^{\widetilde{\mathbf{X}}})$, which suggests that $\lambda = s/n$. Although (in general) $\mathcal{L}_{\mathcal{D}_s,\mathbf{X}}$ is not a lower bound of $\log p(\mathcal{D})$, we found in a practice setting that λ to s/n still results in reasonable performance. However, our theoretical framework gives the reassuring guarantee that if we use full-batch training, we would, in fact, maximize a lower bound of $\log p(\mathcal{D})$. In the following, we present two algorithms, namely Stein functional variational NNs and Stein functional variational gradient boosting (A.2.1), based on the estimated Stein functional variational gradient – i.e., they depend on the score gradient of the functional prior evaluated at $\mathbf{X}$. If there exists no analytical score gradient, we can use a score gradient estimator, as suggested in Sun et al. (2019). This only requires function samples of the prior process evaluated at $\mathbf{X}$, but estimating the score gradient is usually computationally expensive (Zhou et al., 2020). Since our approach builds upon SVGD, there exists an additional approach in our framework based on a gradient-free SVGD (Han & Liu, 2018) that only requires the evaluation of the marginal densities of the prior process.

Stein Functional Variational Neural Network (SFVNN) Sun et al. (2019) proposed to train neural networks (NNs) acting as function generators with the negative functional ELBO as loss, which they call Bayesian Functional Variational Neural Networks (BFVNNs). Such a function generator can be modeled via an NN with stochastic weights, which can be represented as a differentiable function $g : \mathcal{Z} \to \mathcal{Y}, z \mapsto g(z)$, where $z \in \mathcal{Z}$ consists of the deterministic input $\mathbf{x}$ and stochastic inputs, i.e., we can model z as a random variable $z \sim p(z|\mathbf{x})$. These NNs are applicable as long as the reparameterization trick (Kingma & Welling, 2014) can be used, i.e., there exists a random variable $\xi \in \Xi$ with $\xi \sim p(\xi)$ and a differentiable function $h_{\boldsymbol{\phi}} : \mathcal{X} \times \Xi \to \mathcal{Z}$ parametrized by $\boldsymbol{\phi}$ such that $h_{\boldsymbol{\phi}}(\mathbf{x}, \xi) \sim p(z|\mathbf{x})$. With this, we can sample a function by sampling $\xi \sim p(\xi)$ and defining $f_\xi : \mathcal{X} \to \mathcal{Y}, \mathbf{x} \mapsto g(h_{\boldsymbol{\phi}}(\mathbf{x}, \xi))$. In this case, we can write the gradient of Eq. 14 w.r.t. $\boldsymbol{\phi}$ as

$$\begin{aligned}\nabla_{\boldsymbol{\phi}} \mathcal{L}_{\mathcal{D}_s,\mathbf{X}}(Q_{[T]}) = \mathbb{E}_{\xi\sim p(\xi)} &\left[\nabla_{\mathbf{f}_\xi{}^{\widetilde{\mathbf{X}}}} \ell(\mathcal{D}_s, \mathbf{f}_\xi{}^{\widetilde{\mathbf{X}}}) \nabla_{\boldsymbol{\phi}} \mathbf{f}_\xi{}^{\widetilde{\mathbf{X}}}\right] \\ &- \mathbb{E}_{\xi\sim p(\xi)} \left[\left(\nabla_{\mathbf{f}_\xi\mathbf{x}} \log p_{Q_\mathbf{X}}(\mathbf{f}_\xi{}^\mathbf{X}) - \nabla_{\mathbf{f}_\xi\mathbf{x}} \log p_{P_{f_\mathbf{X}}}(\mathbf{f}_\xi{}^\mathbf{X})\right) \nabla_{\boldsymbol{\phi}} \mathbf{f}_\xi{}^\mathbf{X}\right].\end{aligned}$$

This is also the result obtained in Sun et al. (2019), where they then use a score estimator (namely, the spectral stein gradient estimator (SSGE; Shi et al., 2018)) to approximate $\nabla_\mathbf{y} \log p_{Q_\mathbf{X}}(\mathbf{f}_\xi{}^\mathbf{X})$. SSGE scales as $\mathcal{O}(r^3 + r^2(s+M))$ and estimates the score gradient in an RKHS, i.e., the entropy gradient $\nabla_{\mathbf{f}_\xi\mathbf{x}} \log p_{Q_\mathbf{X}}(\mathbf{f}_\xi{}^\mathbf{X})$ and the cross entropy gradient $\nabla_{\mathbf{f}_\xi\mathbf{x}} \log p_{P_{f_\mathbf{X}}}(\mathbf{f}_\xi{}^\mathbf{X})$ are taken in different functional spaces. Our SFVNN is based on the parameter gradient

$$\nabla_{\boldsymbol{\phi}} \mathcal{L}_{\mathcal{D}_s,\mathbf{X}}(Q_{[T]}) = \mathbb{E}_{\xi\sim p(\xi)} \left[\nabla_F \mathcal{L}_{\mathcal{D}_s,\mathbf{X}}(Q_{[T]})\big|_{F=0}(f_\xi)(\mathbf{X}) \cdot \nabla_{\boldsymbol{\phi}} \mathbf{f}_\xi{}^\mathbf{X}\right] - \underbrace{\mathbb{E}_{\mathbf{f}\mathbf{x}\sim Q_\mathbf{X}} \nabla_{\boldsymbol{\phi}} \log p_{Q_\mathbf{X},\phi}(\mathbf{f}^\mathbf{X})}_{=0},$$

where we use the general Stein functional variational gradient from Eq. 16. In contrast to Sun et al. (2019), we thereby directly take the functional gradient of the D_{KL} term in an RKHS, and our score gradients of the prior process are also subject to the implicit kernel smoothing. Hence, our approach scales only quadratically in r, allowing for a larger number of sample functions.

3.4 Illustrative Example

Given three sample functions and two data points $\{(0.75, 1.0), (2.0, 0.0)\}$ (1a), we want to approximate the posterior GP (Figure 1h) w.r.t. the prior GP shown in Figure 1b and a Gaussian likelihood via SFVGB. Hence, we also sample a necessary measure point $x_M = 1.5$. The resulting three-dimensional marginal density is defined by the prior GP. SVGD gives us the optimal update direction for the sample function values to fit this marginal density (Figures 1c, 1d). We fit a kernel

Algorithm 1: Stein Functional Variational Gradient Descent Step `sfvgd_step`

Hyperparameters: Dataset $\mathcal{D}$, log likelihood ℓ, prior SP P_f, number of measure points M, sampling distribution $C_{\mathcal{X}}$ over $\mathcal{X}$, regularization parameter λ
Input: Set of particle functions $\{f_i\}_{i=1}^r$ treated as multi-output function f
Output: Input locations to update $\mathbf{X}$, Stein functional variational gradient (of f evaluated at $\mathbf{X}$) $\mathbf{\Delta_{fX}}$

$\mathbf{X}_M \sim C_{\mathcal{X}}; \mathcal{D}_s = (\widetilde{\mathbf{X}}, \widetilde{\mathbf{y}}) \subset \mathcal{D}$
$\mathbf{X} = \left[\widetilde{\mathbf{X}}, \mathbf{X}_M\right]$
for $j = 1, \dots, r$ **do**
  $\mathbf{\Delta}_{j,\ell} = \frac{1}{r}\sum_{i=1}^r \left[\nabla_{\mathbf{f_i}\widetilde{\mathbf{X}}}\ell(\mathcal{D}_s, \mathbf{f_i}^{\widetilde{\mathbf{X}}})\delta_{\mathbf{f_i}\widetilde{\mathbf{X}}}(\mathbf{f_j}^{\widetilde{\mathbf{X}}})\right] \cdot \left[\delta_{\widetilde{\mathbf{X}}_1}(\cdot), \dots, \delta_{\widetilde{\mathbf{X}}_s}(\cdot)\right]^\top$
  $\mathbf{\Delta}_{j,\mathrm{KL}} = \frac{1}{r}\sum_{i=1}^r \left[\nabla_{\mathbf{f_i}\mathbf{X}} \log p_{P_{f_{\mathbf{X}}}}(\mathbf{f_i}^{\mathbf{X}})k_{\mathbf{Y}}(\mathbf{f_i}^{\mathbf{X}}, \mathbf{f_j}^{\mathbf{X}}) + \nabla_{\mathbf{f_i}\mathbf{X}} k_{\mathbf{Y}}(\mathbf{f_i}^{\mathbf{X}}, \mathbf{f_j}^{\mathbf{X}})\right]$
    $\cdot \left[\delta_{\mathbf{X}_1}(\cdot), \dots, \delta_{\mathbf{X}_{s+M}}(\cdot)\right]^\top$
end
$\mathbf{\Delta_{fX}} = (\mathbf{\Delta}_\ell + \lambda \cdot \mathbf{\Delta}_{\mathrm{KL}})(\mathbf{X})$

Algorithm 2: Stein Functional Variational Neural Network

Hyperparameters: Same as for `sfvgd_step`
Input: Variational posterior $g(\cdot)$, optimizer `opt`
Output: Variational posterior $g(\cdot)$, which approximates the target distribution
while ϕ *not converged* **do**
  $f_i = g(h_{\phi}(\mathbf{X}, \xi_i)), \xi_i \sim p(\xi), \quad i = 1, \dots, r$
  $\mathbf{X}, \mathbf{\Delta_{fX}} = \texttt{sfvgd_step}(f)$
  $\phi = \texttt{opt}(\phi, \mathbf{X}, \mathbf{\Delta_{fX}})$
end

ridge regression to these directions after adding the log likelihood gradients at the two data points (Figure 1e). The resulting updated function samples after this SFVGD step can be seen in Figure 1f and the converged function samples in Figure 1g. Qualitatively comparing these converged sample functions in Figure 1g with sample functions from the exact posterior GP in Figure 1h reassures that we are are able to approximate the posterior GP in this toy example reasonably well.

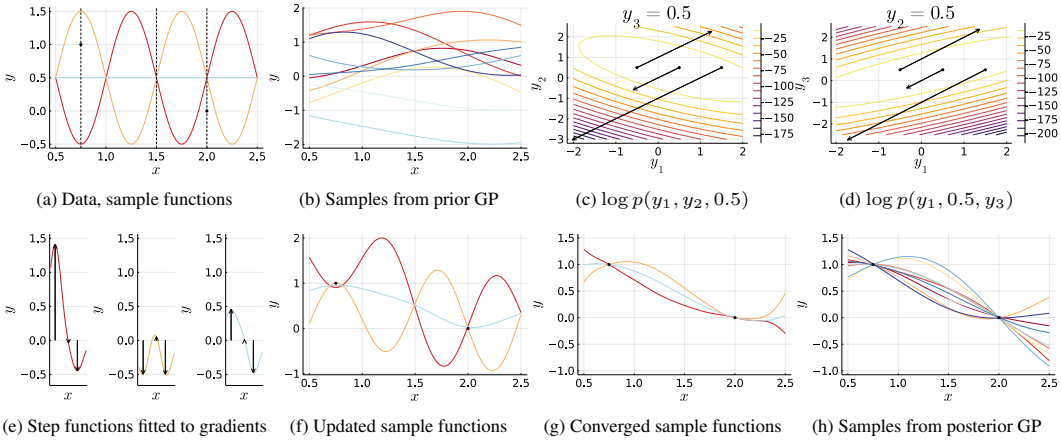

(a) Data, sample functions (b) Samples from prior GP (c) $\log p(y_1, y_2, 0.5)$ (d) $\log p(y_1, 0.5, y_3)$

(e) Step functions fitted to gradients (f) Updated sample functions (g) Converged sample functions (h) Samples from posterior GP

Figure 1: Illustrative example of SFVGB. The points in (a) represent the given data points, and the dashed lines represent all x values that define the marginal prior density in (c,d) w.r.t. the prior GP shown in (b). The arrows in (c) show the resulting SFVGD gradients.

4 Benchmark Study

In addition to simpler examples like the one in the previous subsection, we investigate the usefulness of our approach in a large benchmark study. The main aim is to test the competitiveness of our

Table 1: Comparison of different methods (columns) on all benchmark data sets (rows) using the average NLL (smaller is better) and RMSE over 10 train-test data splits with standard deviation in brackets. The best performing method for each data set is highlighted in bold.

	Test negative log-likelihood			Test root-mean-square error		
	SFVNN	FVBNN	BNN	SFVNN	FVBNN	BNN
Airfoil	**2.10** (0.17)	2.29 (0.04)	2.62 (0.12)	**1.82** (0.20)	1.97 (0.19)	3.40 (0.40)
Concrete	**2.99** (0.19)	3.07 (0.05)	3.25 (0.04)	**4.58** (0.34)	4.64 (0.54)	6.18 (0.34)
Diabetes	5.42 (0.08)	5.49 (0.03)	**5.41** (0.04)	54.57 (3.74)	57.1 (2.48)	**52.7** (2.88)
Energy	**0.62** (0.10)	0.70 (0.09)	2.26 (0.32)	0.44 (0.05)	**0.43** (0.08)	2.37 (0.65)
ForestF	2.38 (0.44)	1.84 (0.05)	**1.83** (0.05)	1.76 (0.31)	**1.51** (0.07)	**1.51** (0.08)
Wine	1.96 (1.45)	1.47 (1.07)	**-0.03** (0.07)	**0.11** (0.02)	0.14 (0.02)	0.21 (0.03)
Yacht	**1.06** (0.30)	1.11 (0.24)	1.35 (0.19)	0.67 (0.26)	**0.61** (0.25)	0.96 (0.28)
GPU	**4.73** (0.04)	4.80 (0.03)	**4.73** (0.02)	27.67 (1.26)	29.6 (0.9)	**27.5** (0.67)
NavalT	**-6.91** (0.06)	-6.85 (0.08)	-5.03 (0.24)	**1.70E-4** (2.5E-5)	1.94E-4 (3.3E-5)	6.50E-4 (6.5E-5)
NavalC	**-6.53** (0.01)	-6.41 (0.05)	-6.44 (0.11)	**1.35E-4** (1.1E-4)	2.39E-4 (3.5E-5)	2.15E-4 (3.9E-5)
Protein	**2.85** (0.01)	2.87 (0.01)	2.96 (0.01)	**4.19** (0.04)	4.27 (0.04)	4.65 (0.05)
VideoMem	11.39 (0.39)	**11.3** (0.10)	11.4 (0.03)	21119 (4910)	**20800** (2320)	21800 (788)
VideoTime	**2.29** (0.05)	2.53 (0.36)	2.86 (1.02)	**2.51** (0.16)	3.14 (0.88)	3.83 (2.08)
Mean rank	1.50	2.15	2.31	1.53	1.96	2.50

approach using its neural network variant (SFVNN) with its closest neighbor, the functional variational Bayesian neural network (FVBNN) from Sun et al. (2019). We also include one well-established BNN approach in our experiments: a BNN using the *Bayes by backprop* principle proposed by Blundell et al. (2015). For results from SVFGB we refer to Section A.2.2 in the Appendix. For most of the datasets, however, the NN provides a better fit to the data. Further experiments and details – in particular, the use of our approach for contextual bandits experiments – can be found in Appendix A.4.

Data and experimental setup We use the benchmark data setup proposed by Hernandez-Lobato & Adams (2015) and Sun et al. (2019) for evaluating probabilistic regression approaches. This setup includes selected data sets from the UCI repository – namely, the four smaller data sets Concrete, Energy, Wine, Yacht, and the four larger data sets Naval, Protein, Video (Memory and Time), and GPU. In addition to Sun et al. (2019), we also compare our approaches on three additional smaller data sets (Airfoil, Diabetes, Forest Fire) and further investigate the second task on the Naval data set (i.e., we examine both the compressor decay and the turbine decay state coefficient, referred to as NavalC and NavalT, respectively). All data sets are standardized prior to model fitting and split into 90% training data and 10% test data for the experiments. For the comparisons, this splitting process is repeated 10 times based on 10 different splits to also evaluate the variability of each method. Further details on data sets, data set-specific pre-processing, and their references can be found in the Appendix.

Details on methods and comparisons In order to provide a fair comparison between methods, we reproduce the best results reported by Sun et al. (2019) for FVBNN and BNN, and also use the same hyperparameters for our method except that while Sun et al. (2019) use $\lambda = 1$, we set λ to s/n. Details for each procedure are given in the Appendix. We compare methods based on the negative log-likelihood (NLL) and the root mean squared error (RMSE) on each test data set and calculate the mean and standard deviation across all 10 data splits.

Results Results are summarized in Table 1, indicating that SFVNN is competitive with other existing approaches for both small and large data sets. As the two functional approaches (SFVNN, FVBNN) optimize the same objective, we would expect them to perform similarly, which is confirmed by the results. We further observe that a weight space approach (the BNN) seems to work better than the functional approaches for a few datasets (in particular, for the Wine dataset, where this is expected as the outcome is of discrete nature).

5 Conclusion

We introduced a novel gradient descent in distribution space that allows us to update a set of particle functions in a general manner to resemble sample functions from a target process. SFVNN was found to be competitive with or to outperform FBVNN while having less computational costs.

REFERENCES

Rafael Ballester-Ripoll, Enrique G. Paredes, and Renato Pajarola. Sobol tensor trains for global sensitivity analysis, 2017.

Charles Blundell, Julien Cornebise, Koray Kavukcuoglu, and Daan Wierstra. Weight uncertainty in neural network. In Francis Bach and David Blei (eds.), *Proceedings of the 32nd International Conference on Machine Learning*, volume 37 of *Proceedings of Machine Learning Research*, pp. 1613–1622, Lille, France, 07–09 Jul 2015. PMLR. URL https://proceedings.mlr.press/v37/blundell15.html.

David R. Burt, Sebastian W. Ober, Adrià Garriga-Alonso, and Mark van der Wilk. Understanding variational inference in function-space, 2020. URL https://arxiv.org/abs/2011.09421.

Tianqi Chen, Emily B. Fox, and Carlos Guestrin. Stochastic gradient hamiltonian monte carlo, 2014. URL https://arxiv.org/abs/1402.4102.

Andrea Coraddu, Luca Oneto, Alessandro Ghio, Stefano Savio, Davide Anguita, and Massimo Figari. Machine learning approaches for improving condition?based maintenance of naval propulsion plants. *Journal of Engineering for the Maritime Environment*, –(–):–, 2014.

Paulo Cortez and Aníbal de Jesus Raimundo Morais. A data mining approach to predict forest fires using meteorological data. 2007.

Francesco D'Angelo and Vincent Fortuin. Repulsive deep ensembles are bayesian, 2021. URL https://arxiv.org/abs/2106.11642.

Francesco D'Angelo, Vincent Fortuin, and Florian Wenzel. On stein variational neural network ensembles, 2021. URL https://arxiv.org/abs/2106.10760.

Dheeru Dua and Casey Graff. UCI machine learning repository, 2017. URL http://archive.ics.uci.edu/ml.

Jun Han and Qiang Liu. Stein variational gradient descent without gradient. In Jennifer Dy and Andreas Krause (eds.), *Proceedings of the 35th International Conference on Machine Learning*, volume 80 of *Proceedings of Machine Learning Research*, pp. 1900–1908. PMLR, 10–15 Jul 2018. URL https://proceedings.mlr.press/v80/han18b.html.

Jose Miguel Hernandez-Lobato and Ryan Adams. Probabilistic backpropagation for scalable learning of bayesian neural networks. In Francis Bach and David Blei (eds.), *Proceedings of the 32nd International Conference on Machine Learning*, volume 37 of *Proceedings of Machine Learning Research*, pp. 1861–1869, Lille, France, 07–09 Jul 2015. PMLR. URL http://proceedings.mlr.press/v37/hernandez-lobatoc15.html.

Alexander Immer, Maciej Korzepa, and Matthias Bauer. Improving predictions of bayesian neural nets via local linearization, 2020. URL https://arxiv.org/abs/2008.08400.

Diederik P. Kingma and Max Welling. Auto-encoding variational bayes. *CoRR*, abs/1312.6114, 2014.

John Lamperti. *Stochastic processes : a survey of the mathematical theory / J. Lamperti.* Applied mathematical sciences (Springer-Verlag New York Inc.); v. 23. Springer-Verlag, New York, 1977. ISBN 0387902759.

Alex Leviyev, Joshua Chen, Yifei Wang, Omar Ghattas, and Aaron Zimmerman. A stochastic stein variational newton method, 2022. URL https://arxiv.org/abs/2204.09039.

Qiang Liu and Dilin Wang. Stein variational gradient descent: A general purpose bayesian inference algorithm. In *Proceedings of the 30th International Conference on Neural Information Processing Systems*, NIPS'16, pp. 2378–2386, Red Hook, NY, USA, 2016. Curran Associates Inc. ISBN 9781510838819.

Chao Ma and José Miguel Hernández-Lobato. Functional variational inference based on stochastic process generators. In M. Ranzato, A. Beygelzimer, Y. Dauphin, P.S. Liang, and J. Wortman Vaughan (eds.), *Advances in Neural Information Processing Systems*, volume 34, pp. 21795–21807. Curran Associates, Inc., 2021. URL https://proceedings.neurips.cc/paper/2021/file/b613e70fd9f59310cf0a8d33de3f2800-Paper.pdf.

Andrey Malinin, Liudmila Prokhorenkova, and Aleksei Ustimenko. Uncertainty in gradient boosting via ensembles. In *International Conference on Learning Representations*, 2021. URL https://openreview.net/forum?id=1Jv6b0Zq3qi.

Alexander G. Matthews, James Hensman, Richard E. Turner, and Zoubin Ghahramani. On sparse variational methods and the kullback-leibler divergence between stochastic processes, 2015.

Carlos Riquelme, George Tucker, and Jasper Snoek. Deep bayesian bandits showdown. In *International Conference on Learning Representations*, 2018.

Tim G. J. Rudner, Zonghao Chen, Yee Whye Teh, and Yarin Gal. Tractable function-space variational inference in bayesian neural networks. 2021.

Mark J. Schervish. *Theory of Statistics*. Springer New York, 1995. doi: 10.1007/978-1-4612-4250-5. URL https://doi.org/10.1007/978-1-4612-4250-5.

Jiaxin Shi, Shengyang Sun, and Jun Zhu. A spectral approach to gradient estimation for implicit distributions, 2018.

Shengyang Sun, Guodong Zhang, Jiaxin Shi, and Roger Grosse. Functional variational bayesian neural networks, 2019. URL https://arxiv.org/abs/1903.05779.

Athanasios Tsanas and Angeliki Xifara. Accurate quantitative estimation of energy performance of residential buildings using statistical machine learning tools. *Energy and buildings*, 49:560–567, 2012.

Dilin Wang, Ziyang Tang, Chandrajit Bajaj, and Qiang Liu. Stein variational gradient descent with matrix-valued kernels, 2019a. URL https://arxiv.org/abs/1910.12794.

Ziyu Wang, Tongzheng Ren, Jun Zhu, and Bo Zhang. Function space particle optimization for bayesian neural networks, 2019b.

I-C Yeh. Modeling of strength of high-performance concrete using artificial neural networks. *Cement and Concrete research*, 28(12):1797–1808, 1998.

Yuhao Zhou, Jiaxin Shi, and Jun Zhu. Nonparametric score estimators. In Hal Daumé III and Aarti Singh (eds.), *Proceedings of the 37th International Conference on Machine Learning*, volume 119 of *Proceedings of Machine Learning Research*, pp. 11513–11522. PMLR, 13–18 Jul 2020. URL https://proceedings.mlr.press/v119/zhou20c.html.

A APPENDIX

A.1 PROOFS

A.1.1 FUNCTIONAL DERIVATIVE OF THE RISK FUNCTIONAL

Assuming that $p(\mathbf{x}, y)L_{(\mathbf{x},y)}[f] \in L^1$ using Fubini's theorem, we find that

$$\mathcal{R}[f] = \mathbb{E}_{(\mathbf{x},y)\sim\mathbb{P}_{\mathbf{x}y}} L_{(\mathbf{x},y)}[f] = \int_{\mathcal{X}\times\mathcal{Y}} p(\mathbf{x}, y)L_{(\mathbf{x},y)}[f]d\mathbf{x}\, dy \tag{19}$$

$$= \int_{\mathcal{X}} \underbrace{p(\mathbf{x}) \int_{\mathcal{Y}} p(y|\mathbf{x})L_{(\mathbf{x},y)}[f]dy}_{=:\mathcal{L}(\mathbf{x},f(\mathbf{x}))}\, d\mathbf{x}. \tag{20}$$

Assuming that $\mathcal{L}$ is sufficiently smooth using the Euler-Lagrange derivative, we find that

$$\nabla_f \mathcal{R}[f](\mathbf{x}) = \frac{\partial\left(\mathcal{L}(\mathbf{x}, f(\mathbf{x}))\right)}{\partial f(\mathbf{x})} \tag{21}$$

$$= p(\mathbf{x}) \int_{\mathcal{Y}} p(y|\mathbf{x}) \frac{\partial L_{(\mathbf{x},y)}[f]}{\partial f(\mathbf{x})} dy \tag{22}$$

$$= p(\mathbf{x}) \cdot \mathbb{E}_{y\sim\mathbb{P}_{y|\mathbf{x}}} \frac{\partial L_{(\mathbf{x},y)}[f]}{\partial f(\mathbf{x})}. \tag{23}$$

A.1.2 FUNCTIONAL DERIVATIVE OF THE FUNCTIONAL ELBO

Let F be an operator that depends on evaluation only with associated maps $F_{\widetilde{\mathbf{X}}} : \mathcal{Y}^s \to \mathcal{Y}^s, F_{\mathbf{X}} : \mathcal{Y}^{s+M} \to \mathcal{Y}^{s+M}$. Further, let $\mathcal{F}[F] = \mathcal{L}_{\mathcal{D}_s,\mathbf{X}}(Q_{[T]}) = \underbrace{\mathbb{E}_{\widetilde{\mathbf{y}}\sim Q_{[T]\widetilde{\mathbf{X}}}} \ell(\mathcal{D}_s, \widetilde{\mathbf{y}})}_{=\mathcal{F}_1[F_{\widetilde{\mathbf{X}}}]} - \underbrace{D_{\mathrm{KL}}(Q_{[T]\mathbf{X}} \| P_{f\mathbf{X}})}_{=\mathcal{F}_2[F_{\mathbf{X}}]}$.
In general, and under the assumption that ℓ is sufficiently smooth, we find that

$$\nabla_{F_{\widetilde{\mathbf{X}}}} \mathcal{F}_1[F_{\widetilde{\mathbf{X}}}] = \nabla_{F_{\widetilde{\mathbf{X}}}} \mathbb{E}_{\widetilde{\mathbf{y}}\sim Q_{\widetilde{\mathbf{X}}}} \ell(\mathcal{D}_s, \widetilde{\mathbf{y}} + F_{\widetilde{\mathbf{X}}}(\widetilde{\mathbf{y}})) = \mathbb{E}_{\widetilde{\mathbf{y}}\sim Q_{\widetilde{\mathbf{X}}}} \left[\nabla_{\widetilde{\mathbf{y}}} \ell(\mathcal{D}_s, \widetilde{\mathbf{y}} + F_{\widetilde{\mathbf{X}}}(\widetilde{\mathbf{y}})) \cdot \delta_{\widetilde{\mathbf{y}}}(\cdot)\right]. \tag{24}$$

Under the assumption that $\mathcal{H}_{\widetilde{\mathbf{Y}}} \subset \{f : \mathcal{Y}^s \to \mathcal{Y}^s\}$ is an RKHS with associated kernels $k_{\widetilde{\mathbf{Y}}}$, we find that

$$\mathcal{F}_1[F_{\widetilde{\mathbf{X}}} + \varepsilon G_{\widetilde{\mathbf{X}}}] - \mathcal{F}_1[F_{\widetilde{\mathbf{X}}}] = \mathbb{E}_{\widetilde{\mathbf{y}}\sim Q_{\widetilde{\mathbf{X}}}} \left[\ell(\mathcal{D}_s, \widetilde{\mathbf{y}} + F_{\widetilde{\mathbf{X}}}(\widetilde{\mathbf{y}}) + \varepsilon G_{\widetilde{\mathbf{X}}}(\widetilde{\mathbf{y}})) - \ell(\mathcal{D}_s, \widetilde{\mathbf{y}} + F_{\widetilde{\mathbf{X}}}(\widetilde{\mathbf{y}}))\right] \tag{25}$$

$$= \varepsilon\, \mathbb{E}_{\widetilde{\mathbf{y}}\sim Q_{\widetilde{\mathbf{X}}}} \left[\nabla_{\widetilde{\mathbf{y}}} \ell(\mathcal{D}_s, \widetilde{\mathbf{y}} + F_{\widetilde{\mathbf{X}}}(\widetilde{\mathbf{y}})) \cdot G_{\widetilde{\mathbf{X}}}(\widetilde{\mathbf{y}})\right] + \mathcal{O}(\varepsilon^2) \tag{26}$$

$$= \varepsilon\, \mathbb{E}_{\widetilde{\mathbf{y}}\sim Q_{\widetilde{\mathbf{X}}}} \left[\nabla_{\widetilde{\mathbf{y}}} \ell(\mathcal{D}_s, \widetilde{\mathbf{y}} + F_{\widetilde{\mathbf{X}}}(\widetilde{\mathbf{y}})) \cdot \langle k_{\widetilde{\mathbf{Y}}}(\widetilde{\mathbf{y}}, \cdot), G_{\widetilde{\mathbf{X}}}\rangle\right] + \mathcal{O}(\varepsilon^2) \tag{27}$$

$$= \varepsilon\, \langle \mathbb{E}_{\widetilde{\mathbf{y}}\sim Q_{\widetilde{\mathbf{X}}}} \left[\nabla_{\widetilde{\mathbf{y}}} \ell(\mathcal{D}_s, \widetilde{\mathbf{y}} + F_{\widetilde{\mathbf{X}}}(\widetilde{\mathbf{y}})) \cdot k_{\widetilde{\mathbf{Y}}}(\widetilde{\mathbf{y}}, \cdot)\right], G_{\widetilde{\mathbf{X}}}\rangle + \mathcal{O}(\varepsilon^2), \tag{28}$$

from which it follows that

$$\nabla_{F_{\widetilde{\mathbf{X}}}} \mathcal{F}_1[F_{\widetilde{\mathbf{X}}}]\big|_{F_{\widetilde{\mathbf{X}}}=0} = \mathbb{E}_{\widetilde{\mathbf{y}}\sim Q_{\widetilde{\mathbf{X}}}} \left[\nabla_{\widetilde{\mathbf{y}}} \ell(\mathcal{D}_s, \widetilde{\mathbf{y}} + F_{\widetilde{\mathbf{X}}}(\widetilde{\mathbf{y}})) \cdot k_{\widetilde{\mathbf{Y}}}(\widetilde{\mathbf{y}}, \cdot)\right]\big|_{F_{\widetilde{\mathbf{X}}}=0} \tag{29}$$

$$= \mathbb{E}_{\widetilde{\mathbf{y}}\sim Q_{\widetilde{\mathbf{X}}}} \left[\nabla_{\widetilde{\mathbf{y}}} \ell(\mathcal{D}_s, \widetilde{\mathbf{y}}) \cdot k_{\widetilde{\mathbf{Y}}}(\widetilde{\mathbf{y}}, \cdot)\right]. \tag{30}$$

Under the assumption that $\mathcal{H}_{\mathbf{Y}} \subset \{f : \mathcal{Y}^{s+M} \to \mathcal{Y}^{s+M}\}$ is an RKHS with associated kernels $k_{\mathbf{Y}}$, it has been shown in Liu & Wang (2016) that

$$\nabla_{F_{\mathbf{X}}} \mathcal{F}_2[F_{\mathbf{X}}]\big|_{F_{\mathbf{X}}=0} = -\mathbb{E}_{\mathbf{y}\sim Q_{\mathbf{X}}} \left[\nabla_{\mathbf{y}} \log p_{P_{f\mathbf{X}}}(\mathbf{y}) k_{\mathbf{Y}}(\mathbf{y}, \cdot) + \nabla_{\mathbf{y}} k_{\mathbf{Y}}(\mathbf{y}, \cdot)\right]. \tag{31}$$

Using the chain rule, we obtain

$$\nabla_F \mathcal{L}_{\mathcal{D}_s,\mathbf{X}}(Q_{[T]})\big|_{F=0}(f) = \nabla_{F_{\widetilde{\mathbf{X}}}} \mathcal{F}_1[F_{\widetilde{\mathbf{X}}}](\mathbf{f}^{\widetilde{\mathbf{X}}}) \nabla_F \left[F_{\widetilde{\mathbf{X}}}\right](f)\Big|_{F=0} \tag{32}$$

$$- \nabla_{F_{\mathbf{X}}} \mathcal{F}_2[F_{\mathbf{X}}](\mathbf{f}^{\mathbf{X}}) \nabla_F \left[F_{\mathbf{X}}\right](f)\Big|_{F=0}. \tag{33}$$

$$\tag{34}$$

Algorithm 3: Stein Functional Variational Gradient Boosting

Hyperparameters: Same as for `sfvgd_step`
Input: number of iterations $t_{\max}$, learning rate $\eta^{[t]}$ in the t-th iteration, set of initial particle functions $\{f_i^{[0]}\}_{i=1}^r$ treated as multi-output function $f^{[0]}$, multi-output base learner $\mathcal{I}_b$
Output: Set of particle functions $\{f_i^{[t_{\max}]}\}_{i=1}^r$, which approximate the target distribution
for $t = 0, \dots, t_{\max} - 1$ **do**
  $\mathbf{X}, \mathbf{\Delta_f x} = \texttt{sfvgd_step}(f^{[t]})$
  $f^{[t+1]} = f^{[t]} + \eta^{[t]} \cdot \mathcal{I}_b(\mathbf{X}, \mathbf{\Delta_f x})$
end

Table 2: Results of SFVGB (rows) on the small benchmark data sets (columns) using the average NLL (smaller is better) and RMSE over 10 train-test data splits with standard deviation in brackets. The best performing method for each data set is highlighted in bold.

	Airfoil	Concrete	Diabetes	Energy	ForestF	Wine	Yacht
RMSE	3.31 (0.26)	6.71 (0.52)	57.83 (0.67)	1.93 (0.14)	1.53 (0.07)	0.18 (0.04)	4.83 (1.24)
NLL	2.87 (0.18)	3.41 (0.13)	7.04 (0.67)	2.16 (0.10)	6.31 (0.69)	2.37 (2.00)	3.21 (0.52)

Since F is evaluation-only dependent, we observe that $\nabla_F \left[F_{\{\mathbf{x}\}}\right](f) = \delta_{\mathbf{x}}(\cdot)$ and conclude that

$$\nabla_F \mathcal{L}_{\mathcal{D}_s,\mathbf{X}}(Q_{[T]})\big|_{F=0}(f) = \nabla_{F_{\widetilde{\mathbf{X}}}} \mathcal{F}_1[F_{\widetilde{\mathbf{X}}}](\mathbf{f}^{\widetilde{\mathbf{X}}})\Big|_{F_{\widetilde{\mathbf{X}}}=0} \cdot \left[\delta_{\widetilde{\mathbf{X}}_1}(\cdot), \dots, \delta_{\widetilde{\mathbf{X}}_s}(\cdot)\right]^\top \tag{35}$$

$$- \nabla_{F_{\mathbf{X}}} \mathcal{F}_2[F_{\mathbf{X}}](\mathbf{f}^{\mathbf{X}})\Big|_{F_{\mathbf{X}}=0} \cdot \left[\delta_{\mathbf{X}_1}(\cdot), \dots, \delta_{\mathbf{X}_{s+M}}(\cdot)\right]^\top . \tag{36}$$

If $\mathcal{H}$ is assumed to be an RKHS with associated kernel $k_{\mathcal{X}}(\mathbf{x}, \cdot)$ then this becomes

$$\nabla_F \mathcal{L}_{\mathcal{D}_s,\mathbf{X}}(Q_{[T]})\big|_{F=0}(f) = \nabla_{F_{\widetilde{\mathbf{X}}}} \mathcal{F}_1[F_{\widetilde{\mathbf{X}}}](\mathbf{f}^{\widetilde{\mathbf{X}}})\Big|_{F_{\widetilde{\mathbf{X}}}=0} \cdot \left[k_{\mathcal{X}}(\widetilde{\mathbf{X}}_1, \cdot), \dots, k_{\mathcal{X}}(\widetilde{\mathbf{X}}_s, \cdot)\right]^\top \tag{37}$$

$$- \nabla_{F_{\mathbf{X}}} \mathcal{F}_2[F_{\mathbf{X}}](\mathbf{f}^{\mathbf{X}})\Big|_{F_{\mathbf{X}}=0} \cdot \left[k_{\mathcal{X}}(\mathbf{X}_1, \cdot), \dots, k_{\mathcal{X}}(\mathbf{X}_{s+M}, \cdot)\right]^\top . \tag{38}$$

A.2 SFVGB

A.2.1 SFVGB ALGORITHM

We treat the r particle functions mapping from $\mathcal{X}$ to $\mathcal{Y}$ as a single function $f^{[0]}$ mapping from $\mathcal{X}$ to $\mathcal{Y}^r$ – i.e., we identify the i-th sample function $f_i^{[0]}, i = 1, \dots, r$ with the i-th component of $f^{[0]}$. Analogously to standard GB, we choose a base learner $\mathcal{I}_b$ which defines a hypothesis space $\mathcal{H} \subset \{f : \mathcal{X} \to \mathcal{Y}^r\}$. While this requires the base learner $\mathcal{I}_b$ to be a multi-output learner, it is always possible to use an ensemble of single-output learners. With this, SFVGB is vanilla GB of a multi-output function f where the loss is the negative functional ELBO. Consequently, we update $f^{[t]}$ in the t-th iteration via

$$f^{[t+1]} = f^{[t]} + \eta^{[t]} \mathcal{I}_b\Big(\mathbf{X}, \left[\widetilde{\nabla}_F \mathcal{L}_{\mathcal{D}_s,\mathbf{X}}(Q_{[T]})\big|_{F=0}(f_1^{[t]})(\mathbf{X}), \dots, \widetilde{\nabla}_F \mathcal{L}_{\mathcal{D}_s,\mathbf{X}}(Q_{[T]})\big|_{F=0}(f_r^{[t]})(\mathbf{X})\right]^\top\Big),$$

using Eq. 18 and a (potentially adaptive) learning rate $\eta^{[t]}$.

A.2.2 SFVGB REGRESSION EXPERIMENTS

We also tested SFVGB on the small regression datasets. As the learner, we used a Nadaraya-Watson kernel regression variant, which does not scale the resulting sum of kernel functions. This is the natural learner if the hypothesis space $\mathcal{H}$ is assumed to be an RHKS, as discussed in section 2.1. The hyperparemeters of the SFVGD step are the same as ones we used for SFVNN. The results after 1000 iterations are summarized in table 2.

Table 3: Data set characteristics, additional pre-processing and references.

Dataset	# Obs.	# Feat.	Pre-processing	Reference
Airfoil	1503	5	-	Dua & Graff (2017)
Concrete	1030	8	-	Yeh (1998)
Diabetes	442	10	-	Dua & Graff (2017)
Energy	768	8	-	Tsanas & Xifara (2012)
ForestF	517	12	logp1 transformation for `area`; numerical representation for `month` and `day`	Cortez & Morais (2007)
Wine	178	13	-	Dua & Graff (2017)
Yacht	308	6	-	Dua & Graff (2017)
GPU	241600	14	only use run 1 as outcome	Ballester-Ripoll et al. (2017)
NavalT	11934	15	drop features with zero variance	Coraddu et al. (2014)
NavalC	11934	15	drop features with zero variance	Coraddu et al. (2014)
Protein	45730	9	-	Dua & Graff (2017)
Video	68784	19	drop highly correlated features; drop `id` and `b_size`; use dummy-coding for `codec` and `o_codec`	Dua & Graff (2017)

A.3 Numerical experiments: further details

A.3.1 Further data details

In Table 3, the data characteristics and pre-processing steps are listed.

A.3.2 Further experimental details

BNN approaches are fitted using the recommended architecture and tuning parameters by Sun et al. (2019). We reduced the epochs from 10,000 to 1,000 epochs for the smaller data sets to reduce the computational runtime. This did not negatively impact the BNN's performance. In all our benchmark experiments, we follow the setup for BNNs and FVBNNs described by Sun et al. (2019).

A.4 Further results

Here, we provide further results using the application of probabilistic methods for contextual bandits.

Contextual Bandits One important application of uncertainty-aware models is for exploration, as in Bayesian optimization, reinforcement learning, or bandits. Following Sun et al. (2019), we evaluate SFVNN using the contextual bandits benchmark by Riquelme et al. (2018) by re-runing the settings investigated in Sun et al. (2019) and report the cumulative regret based on the best expected reward. Following Riquelme et al. (2018), we use the benchmark data sets Adult, Census, Covertype, Financial, Jester, Mushroom, Statlog, and Wheel. For these, the rewards are deterministic, and the regret is equal to the best realized reward. As in previous works, we report the regret as a relative value, relative to a random uniform sampling procedure that emulates Thompson Sampling (see Riquelme et al., 2018). As comparison methods, we use the BNN (with 50 and 500 units), three spinnoffs of the NeuralLinear algorithm (namely, the Bootstrapped NN trained with RMSprop (BootRMS), Parameter Noise (ParamNoise), and Dropout (see Riquelme et al., 2018, for more details)), as well as two variants of the FVBNN (with one and three layers each with 50 units). Experiments are run 5 times with shuffled contexts, for which we report mean and standard deviation of the relative cumulative regret.

Results are given in Table 4, suggesting that both FVBNN and SFVBNN are well- and particularly similar-performing methods in the application of contextual bandits.

Table 4: Relative contextual bandits regret (relative to the cumulative regret of Uniform sampling) for different data sets (columns) and methods (rows). Numbers in brackets of methods indicate the network sizes. Reported numbers are the mean (and standard derivation in brackets) over 5 trials. The best algorithms per data set are highlighted in bold.

	Adult	Census	Covertype	Jester	Mushroom	Statlog	Wheel
BNN (50)	95.79 (1.33)	66.12 (5.10)	61.18 (1.91)	83.70 (3.31)	7.81 (9.39)	29.2 (4.05)	82.94 (22.2)
BNN (500)	99.16 (1.47)	94.38 (11.9)	74.55 (7.32)	79.08 (5.84)	9.31 (11.1)	64.5 (13.3)	**8.892** (15.0)
BootRMS	82.74 (8.16)	53.40 (18.0)	36.95 (10.3)	63.3 (10.74)	7.11 (5.61)	1.81 (2.70)	119.16 (3.7)
Dropout	85.46 (4.74)	37.27 (12.3)	39.55 (5.84)	65.11 (9.62)	4.43 (6.83)	2.89 (4.26)	28.61 (12.1)
FVBNN (50, 50, 50)	72.84 (11.5)	30.46 (28.4)	**24.29** (14.7)	50.45 (20.0)	2.92 (10.3)	3.46 (3.75)	13.62 (14.7)
FVBNN (50)	75.05 (7.66)	40.65 (14.9)	46.57 (3.99)	57.28 (17.8)	**2.39** (6.24)	**1.58** (2.09)	24.24 (22.0)
ParamNoise	89.00 (5.24)	57.86 (15.5)	48.18 (9.84)	66.52 (13.1)	6.74 (5.89)	7.69 (3.57)	21.93 (15.4)
SFVNN (50, 50, 50)	**71.99** (7.29)	36.65 (30.3)	28.47 (16.4)	**50.09** (21.2)	7.81 (9.35)	4.52 (4.12)	44.12 (27.7)
SFVNN (50)	79.62 (5.44)	**30.05** (13.1)	29.24 (11.4)	55.61 (18.0)	6.88 (7.99)	4.01 (2.19)	91.95 (33.2)
Uniform Sampling	100.0 (0.00)	100.0 (0.00)	100.0 (0.00)	100.0 (0.00)	100.0 (0.00)	100.0 (0.00)	100.0 (0.00)